

## Ultrathin lead oxide film on Pb(111) and its application in single spin detection

Ying-Shuang Fu,<sup>1,2</sup> Shuai-Hua Ji,<sup>1,2</sup> Tong Zhang,<sup>1,2</sup> Xi Chen,<sup>2</sup> Xu-Cun Ma,<sup>1</sup> Jin-Feng Jia,<sup>2</sup> and Qi-Kun Xue<sup>2,a)</sup>

<sup>1</sup>*Institute of Physics, Chinese Academy of Sciences, Beijing 100080, People's Republic of China*

<sup>2</sup>*Department of Physics, Tsinghua University, Beijing 100084, People's Republic of China*

(Received 26 May 2009; accepted 25 July 2009; published online 12 August 2009)

The morphology and electronic structure of ultrathin PbO films on silicon-supported Pb islands have been investigated with a low temperature scanning tunneling microscope. It is found that the PbO film acts as an insulating layer to electronically decouple the adsorbates from the metallic substrate. Due to the increased lifetime of spin excitation, the Zeeman splitting of individual manganese phthalocyanine molecules adsorbed on PbO could be detected with spin-flip inelastic tunneling spectroscopy. The ultrathin insulating films like PbO provide an effective way to control the electronic coupling in the nanometer scale. © 2009 American Institute of Physics.

[DOI: 10.1063/1.3205118]

Insulating thin films on metals are of great importance for the applications in the miniaturization of microelectronics, magnetoelectronic devices, and heterogeneous catalysis.<sup>1,2</sup> Interestingly, the adsorbed atoms/molecules on the ultrathin insulating films are significantly decoupled from the metallic substrate, while still accessible by scanning tunneling microscopy (STM) and spectroscopy (STS).<sup>3-6</sup> The ultrathin insulators allowed for single molecule fluorescence,<sup>7</sup> single atom/molecule charging,<sup>8-12</sup> single-spin-flip spectroscopy<sup>13-17</sup> and direct imaging of inherent molecular orbitals.<sup>18,19</sup> However, the ultrathin insulator systems that can be used for these studies are still very limited.

Here, we report a systematic STM/STS study of ultrathin PbO films epitaxially grown on Pb(111) surface. We find that the bilayer PbO films with well-ordered structure suppress the electron density of states over a large range of energy around the Fermi level, and efficiently decouple the adsorbates from the metallic substrate. As a result of such decoupling capability, spin-flip spectroscopy of single molecules adsorbed on PbO could be realized.

The experiments were conducted in a Unisoku UHV <sup>3</sup>He STM system that can reach a base temperature of 0.4 K by means of a single-shot <sup>3</sup>He cryostat. Magnetic field up to 11 T can be applied perpendicular to the sample surface. The Si(111) substrate (*p*-type with a resistivity of 0.2 Ω cm) was cleaned using the standard procedure of current heating at a base pressure of  $1 \times 10^{-10}$  Torr. Pb islands were prepared by depositing 7–8 ML of Pb followed by annealing at room temperature for 30 min. Because of its flat-top geometry,<sup>20</sup> the thickness of a Pb island varies by one atomic layer on every successive silicon terrace.

On the Pb(111) surface, PbO films were prepared by a two-step approach:<sup>21</sup> (i) low-temperature ( $\sim 90$  K) O<sub>2</sub> adsorption at a pressure of  $2 \times 10^{-7}$  Torr for 90 s, followed by annealing at room temperature for 2 h to form (oxidized) nucleation centers and (ii) room-temperature oxidation with an O<sub>2</sub> pressure of  $5 \times 10^{-7}$  Torr for 20 min. A polycrystalline PtIr tip was used in the experiments.

The STM image in Fig. 1(a) shows the typical surface geometry of the PbO islands formed on Pb(111) surface. The PbO islands have two different apparent heights above the Pb surface at a bias voltage of 0.5 V: 0.38 nm for PbO-I (2 ML above Pb) and 0.12 nm for PbO-II (1 ML above Pb), respectively. The apparent height generally depends on the bias voltage. Due to the diffusion of Pb atoms during oxidation, additional layer of Pb [labeled by Pb\* in Fig. 1(a)] appears on the top of the Pb(111) surface.

The image with atomic resolution [Fig. 1(b)] for PbO shows that the PbO film has a rectangular lattice structure with lattice constants of 0.51 and 0.59 nm,<sup>22</sup> respectively. The stripes in the image of PbO are attributed to the Moiré patterns originated from the overlapping between the rectangular lattice of PbO and the triangular lattice of the underlying Pb(111) substrate.

The electronic structure of PbO films was characterized with low temperature STS. Figure 1(c) shows the typical  $dI/dV$  spectrum of PbO grown on 14 ML Pb. Between  $-3$  and 1.8 V, the spectrum is flat with small differential conductance. Although the tunneling electrons can still penetrate the insulating layer, the electron density of states is greatly sup-

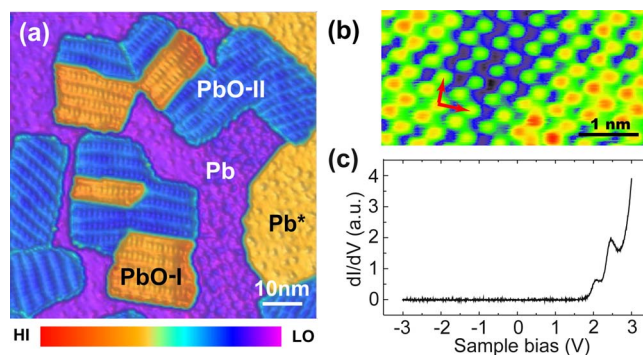


FIG. 1. (Color online) PbO islands on Pb(111) film. (a) A typical STM image of PbO on Pb(111) surface ( $V=0.5$  V and  $I=0.1$  nA). Two different types of PbO islands are labeled by PbO-I and PbO-II. (b) Atomic resolution image of PbO ( $V=0.24$  V and  $I=0.1$  nA). The basal vectors of the two-dimensional lattice are indicated by arrows. (c) Typical STS of a PbO island. The tunneling gap was set by  $V=2.21$  V and  $I=0.86$  nA.

<sup>a)</sup>Electronic mail: qkxue@mail.tsinghua.edu.cn.

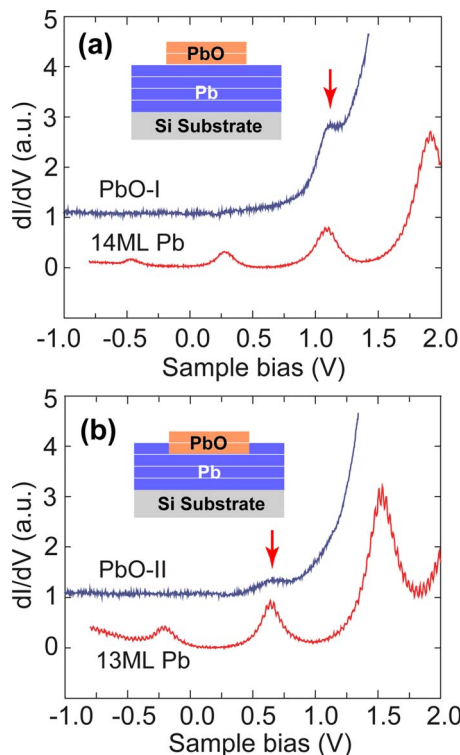


FIG. 2. (Color online) The quantum well states on PbO. (a) The differential conductance measured on PbO-I and 14 ML of Pb. The tunneling conditions:  $V=1.0$  V and  $I=0.1$  nA. (b) The differential conductance measured on PbO-II and 13 ML of Pb. The quantum well states are indicated by arrows. The insets show the growth modes of PbO-I and PbO-II.

pressed within the energy gap of PbO films. The onset for the conduction band of PbO appears at 1.8 V, where  $dI/dV$  starts to increase. The two peaks at 2.07 and 2.46 V are attributed to the bands of PbO with mainly  $6p$  character of Pb.<sup>23,24</sup> It is also noted that the  $dI/dV$  spectra on both PbO-I and PbO-II are essentially the same if the tip-sample separation is large enough.

The thickness of the PbO islands can be determined by the electronic features within the energy gap of PbO. By moving the STM tip closer to the oxide surface, additional peaks in  $dI/dV$  are revealed at 1.16 V [PbO-I, Fig. 2(a)] and 0.66 V [PbO-II, Fig. 2(b)], respectively. These features are attributed to the quantum-well states (QWSs) of the underlying Pb film, which are detectable on oxide at small tip-sample separation. The QWSs are formed in Pb film due to the strong quantum confinement of electron motion along the film normal direction.<sup>21,25,26</sup> The energy spectra of the QWSs depend on and can be utilized to determine the thickness of Pb film. By comparing the electronic structure on oxide with the QWSs on bare Pb film surface (Fig. 2), the thicknesses of the Pb film below PbO-I and PbO-II are found to be 14 and 13 ML, respectively. Therefore, as shown in the insets of Fig. 2, both PbO-I and PbO-II are in fact 2 ML thick while PbO-II has one atomic layer imbedded in the underlying Pb substrate. The above analysis is consistent with the double-layer PbO massicot structure model used to explain the autocatalytic oxidation behavior of lead crystallite surfaces.<sup>22</sup>

The ultrathin insulating films decouple the adsorbates electronically from the metallic substrate and allow the study of the inherent electronic properties of the adsorbed molecules. To demonstrate the decoupling capability of the double-layer PbO, we measured the spin excitations of single

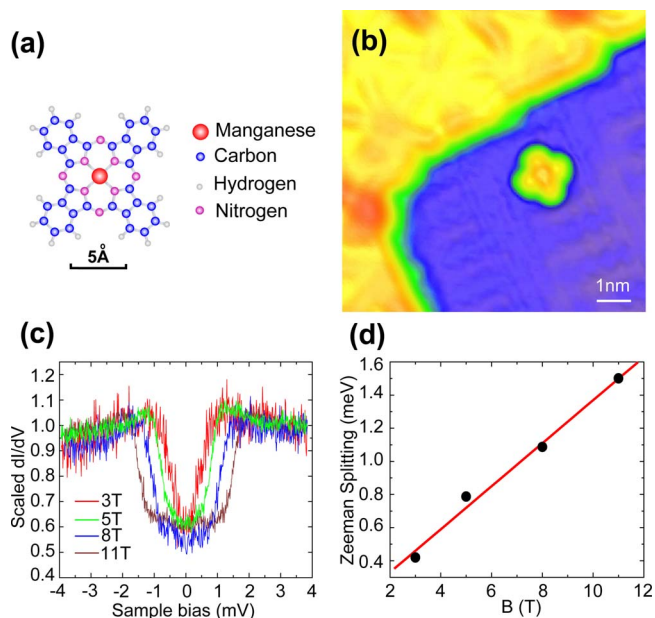


FIG. 3. (Color online) Spin-flip IETS of MnPc molecules on oxide. (a) The schematic molecular structure of MnPc. (b) STM image of a single MnPc molecule on PbO surface ( $V=0.1$  V and  $I=0.1$  nA). (c) Zeeman splitting for a MnPc molecule at different magnetic fields. For all spectra,  $T=0.4$  K. The tunneling gap was set by  $V=6$  mV and  $I=0.2$  nA. The bias modulation was 0.05 mV (rms) at 1991 Hz. (d) Magnetic field dependence of the Zeeman energy in (c). The linear fitting gives the  $g$  factor.

manganese phthalocyanine (MnPc) molecule in magnetic field. Similar to the various insulating layers used in the past studies,<sup>13-17</sup> PbO serves as a buffer to prevent the spins above it from being quenched by the metallic substrate and increase the lifetime of spin excitations.

The spin excitations were measured by the spin-flip inelastic electron tunneling spectroscopy (IETS) with STM,<sup>13-17</sup> which provides an effective way to study single spin. Above a threshold bias voltage at  $\pm\Delta/e$  (where  $\Delta$  is the Zeeman energy and  $-e$  is the charge on an electron), the tunneling electrons may transfer energy to the spin degree of freedom of individual molecules. The threshold is represented by a steplike increase in  $dI/dV$  at  $\pm\Delta/e$ .

A MnPc molecule [Fig. 3(a)] consists of a stable  $\pi$ -conjugated macrocyclic ligand and a  $Mn^{2+}$  ion located at the center. The molecules (Aldrich Inc.) were thermally sublimed onto the surface at room temperature. They tend to adsorb on the metallic Pb surface. Upon adsorption, the magnetic moment of MnPc is reduced from  $3\mu_B$  of an isolated molecule to  $0.99\mu_B$  and further screened by the Kondo effect.<sup>26</sup> To observe the spin-flip IETS, the molecules have to be decoupled from the metallic substrate by moving MnPc onto the oxide with an STM tip. The manipulation could be easily achieved if Pb and PbO have similar heights, i.e., between PbO-II and Pb\*. Figure 3(b) shows the image of a MnPc molecule on PbO. The spin-flip IETS is indicated by the symmetric steps around Fermi level in  $dI/dV$  [Fig. 3(c)]. The Zeeman splitting  $\Delta=g\mu_B B$ , where  $\mu_B$  is the Bohr magneton and  $g$  is the Landé  $g$ -factor, allows the spin-flip excitation at an energy proportional to the applied magnetic field  $B$ . To completely quench the superconducting state of Pb, the magnetic field used in the experiments was above 3 T. A linear fitting of the Zeeman splitting as a function of the magnetic field yields a  $g$ -factor of 2.25 [Fig. 3(d)] for a MnPc molecule on PbO surface. The  $g$ -factor deviates no-

ticeably from that of a free electron and a MnPc molecule directly absorbed on Pb (Ref. 26) due to the local chemical environment of the Mn ion, similar to the discussion in the context of electron paramagnetic resonance.

In summary, we have prepared PbO ultrathin films on Pb(111) surface. The morphology and electronic structure of PbO film were investigated by STM and STS. The insulating oxide layers suppress the electron density of states around the Fermi level. We demonstrate that the adsorbates on PbO are effectively decoupled from the metallic substrate as been in the spin-flip IETS of a single MnPc molecule on PbO.

- <sup>1</sup>S. Schintke and W.-D. Schneider, *J. Phys.: Condens. Matter* **16**, R49 (2004).
- <sup>2</sup>S. A. Chambers, *Surf. Sci. Rep.* **39**, 105 (2000).
- <sup>3</sup>S. Schintke, S. Messerli, M. Pivetta, F. Patthey, L. Liviouille, M. Stengel, A. D. Vita, and W.-D. Schneider, *Phys. Rev. Lett.* **87**, 276801 (2001).
- <sup>4</sup>K. H. Hansen, T. Worren, E. Lægsgaard, F. Besenbacher, and I. Stensgaard, *Surf. Sci.* **475**, 96 (2001).
- <sup>5</sup>J. Repp and G. Meyer, *Appl. Phys. A: Mater. Sci. Process.* **85**, 399 (2006).
- <sup>6</sup>C. D. Ruggiero, T. Choi, and J. A. Gupta, *Appl. Phys. Lett.* **91**, 253106 (2007).
- <sup>7</sup>X. H. Qiu, G. V. Nazin, and W. Ho, *Science* **299**, 542 (2003).
- <sup>8</sup>J. Repp, G. Meyer, F. E. Olsson, and M. Persson, *Science* **305**, 493 (2004).
- <sup>9</sup>S. W. Wu, N. Ogawa, and W. Ho, *Science* **312**, 1362 (2006).
- <sup>10</sup>F. E. Olsson, S. Paavilainen, M. Persson, J. Repp, and G. Meyer, *Phys. Rev. Lett.* **98**, 176803 (2007).
- <sup>11</sup>M. Sterrer, T. Risse, U. M. Pozzoni, L. Giordano, M. Heyde, H.-P. Rust, G. Pacchioni, and H.-J. Freund, *Phys. Rev. Lett.* **98**, 096107 (2007).
- <sup>12</sup>L. Giordano, G. Pacchioni, J. Goniakowski, N. Nilius, E. D. L. Rienks, and H.-J. Freund, *Phys. Rev. Lett.* **101**, 026102 (2008).
- <sup>13</sup>A. J. Heinrich, J. A. Gupta, C. P. Lutz, and D. M. Eigler, *Science* **306**, 466 (2004).
- <sup>14</sup>C. F. Hirjibehedin, C. P. Lutz, and A. J. Heinrich, *Science* **312**, 1021 (2006).
- <sup>15</sup>C. F. Hirjibehedin, C.-Y. Lin, A. F. Otte, M. Ternes, C. P. Lutz, B. A. Jones, and A. J. Heinrich, *Science* **317**, 1199 (2007).
- <sup>16</sup>X. Chen, Y. S. Fu, S. H. Ji, T. Zhang, P. Cheng, X. C. Ma, X. L. Zou, W. H. Duan, J. F. Jia, and Q. K. Xue, *Phys. Rev. Lett.* **101**, 197208 (2008).
- <sup>17</sup>N. Tsukahara, K. Noto, M. Ohara, S. Shiraki, N. Takagi, Y. Takata, J. Miyawaki, A. Chainani, S. Shin, and M. Kawai, *Phys. Rev. Lett.* **102**, 167203 (2009).
- <sup>18</sup>J. Repp, G. Meyer, S. M. Stojkovic, A. Gourdon, and C. Joachim, *Phys. Rev. Lett.* **94**, 026803 (2005).
- <sup>19</sup>J. Repp, G. Meyer, S. Paavilainen, F. E. Olsson, and M. Persson, *Science* **312**, 1196 (2006).
- <sup>20</sup>L. Y. Ma, L. Tang, Z. L. Guan, K. He, K. An, X. C. Ma, J. F. Jia, Q. K. Xue, Y. Han, S. Huang, and F. Liu, *Phys. Rev. Lett.* **97**, 266102 (2006).
- <sup>21</sup>X. C. Ma, P. Jiang, Y. Qi, J. F. Jia, Y. Yang, W. H. Duan, W. X. Li, X. H. Bao, S. B. Zhang, and Q. K. Xue, *Proc. Natl. Acad. Sci. U.S.A.* **104**, 9204 (2007).
- <sup>22</sup>K. Thürmer, E. Williams, and J. Reutt-Robey, *Science* **297**, 2033 (2002).
- <sup>23</sup>H. J. Terpstra, R. A. de Groot, and C. Hass, *Phys. Rev. B* **52**, 11690 (1995).
- <sup>24</sup>D. J. Payne, R. G. Egddell, A. Walsh, G. W. Watson, J. Guo, P.-A. Glans, T. Learmonth, and K. E. Smith, *Phys. Rev. Lett.* **96**, 157403 (2006).
- <sup>25</sup>T.-C. Chiang, *Surf. Sci. Rep.* **39**, 181 (2000).
- <sup>26</sup>Y. S. Fu, S. H. Ji, X. Chen, X. C. Ma, R. Wu, C. C. Wang, W. H. Duan, X. H. Qiu, B. Sun, P. Zhang, J. F. Jia, and Q. K. Xue, *Phys. Rev. Lett.* **99**, 256601 (2007).